

# PHY407 Lab9

Genevieve Beauregard (1004556045)

Anna Shirkalina (1003334448)

Oct 2020

## Question 1

a)

We are asked to use the Crank-Nicolson method to solve the time-dependant Schrodinger equation in an infinitely square well potential. We start by defining all of the necessary constants for the implementation. We then building a Hamiltonian matrix using equations 14 from the lab manual, and initialize  $\Psi$  as specified in equation 13 of the manual. In order to avoid calculation  $\psi_0$  in equation 13 we just normalize `Psi_init` using our `normalize_psi` function which calculates the integral of  $\psi^*\psi$  over  $[-L/2, L/2]$  using the trapezoid integration method. We then define the L and R matrix as specified in equation 17, and then complete the Crank-Nicolson protocol by solving for  $\Psi^{n+1}$  in equation 17. To assure ourselves that the Crank-Nicolson method is stable we calculate the energy at every time step of our integration, we integrate the integrand described by equation 4 in lab manual. As well as calculating equation 3 (without prior re-normalization of  $\Psi$ ) to assure ourselves that the wave function continues to be normalized. When plotting our energy function we choose to plot only the real values since the imaginary part is  $10^{-14}$  times smaller and can be attributed to computer error.

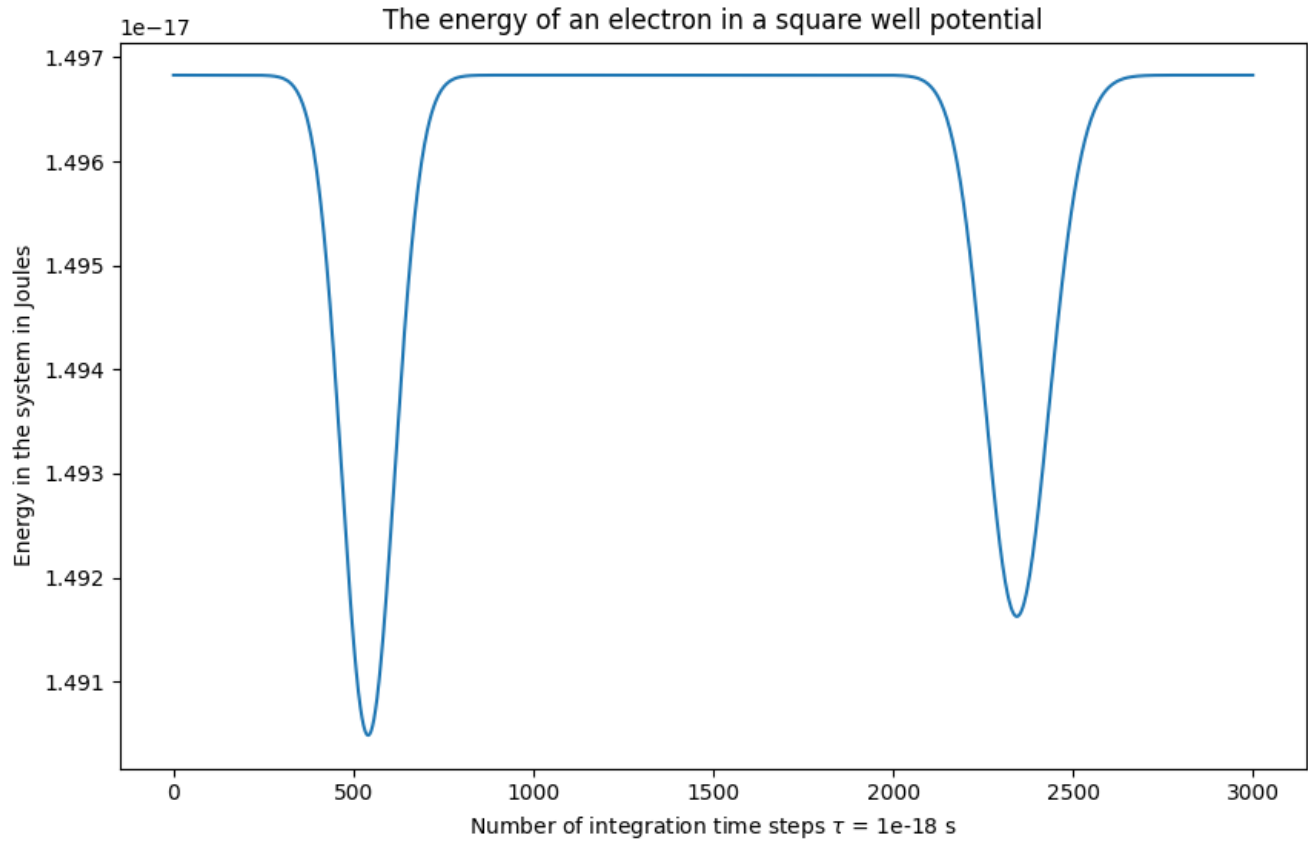


Figure 1: The energy in the system through time in a square well potential.

We observe in figure 1 the energy being constant throughout time with the exceptions of two dips integration steps 500 and 2500. This coincides with the local maximum/minimums in the trajectory as shown in fig 3.

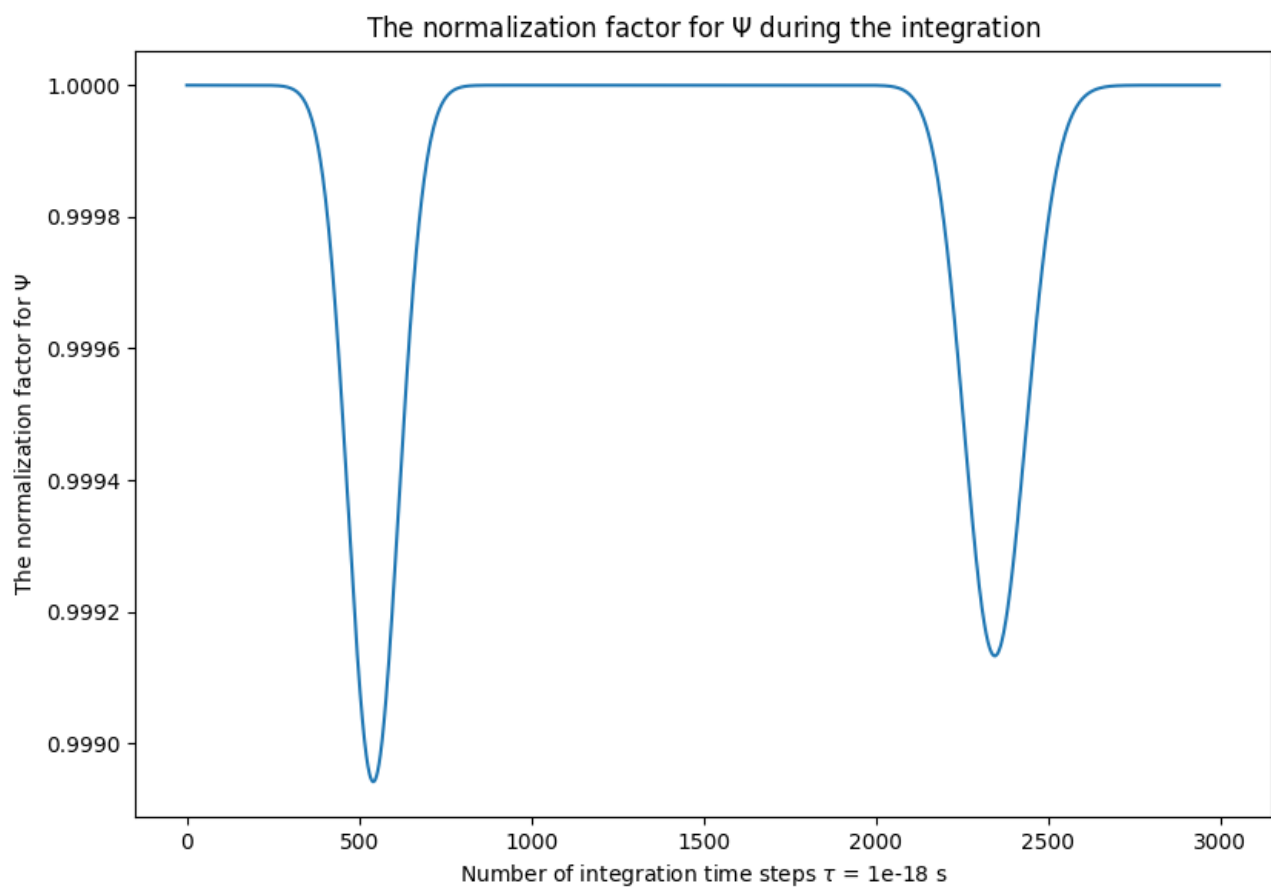


Figure 2: The normalization of the wave function through time in a square well potential.

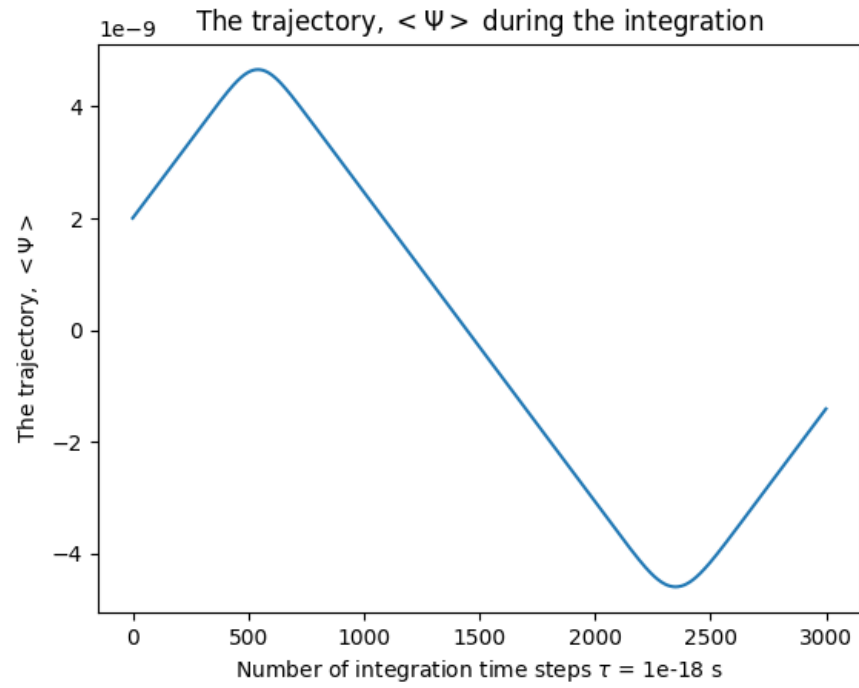


Figure 3: The trajectory of the wave function through time in a square well potential.

The probability density functions for 3000 time steps with  $\tau=1e-18$

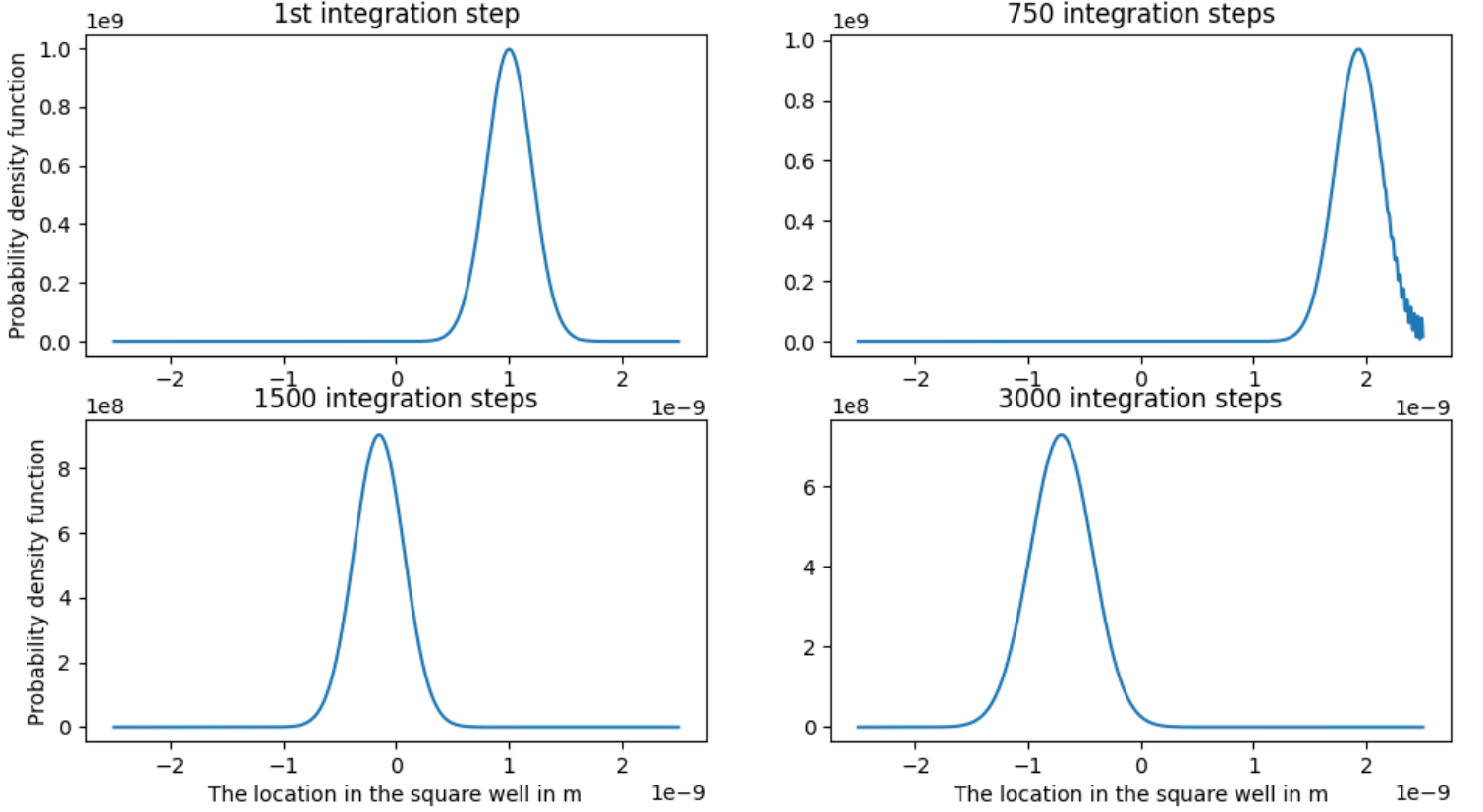


Figure 4: Snapshots of the probability density function for the position in a square well potential.

b)

We examine the probability density function of position, figure 4 and observe a narrow Gaussian distribution. The Gaussian distribution begins in the center of the well moving right, when it hits the right edge of the well at approximately integration step 600 magnitude of the maximum point grows as the width gets smaller. The probability density function then reflects off of the wall similar to the way as wave in a string reflects after a loose end and begins to travel in the opposite direction. The quote from the Ehrenfest theorem suggests that in the case where the wave function is concentrated around some point (such as this case with a Gaussian distribution), we can expect the expected momentum and expected positions will follow the classical trajectories. We can see in figure 3

that the expected position has a classical trajectory of a ball in a well where it is oscillating from one end of the well to the other with constant speed.

**c)**

We are asked to modify our code to calculate the Schrodinger equation with a harmonic oscillator potential, which we do with minimal additional modifications to the code. We observe the trajectory of the wave function in figure 7 which appears a sinusoidal graph. The corresponding energy graph in figure 6 shows that the energy dips every time the trajectory is at a critical point just as we saw in part a. Examining our probability density function in figure 8 we notice that we have sharp concentration for each time step around some point, and the concentration moves through time. This leads us to the conclusion that expectation in position behaves classically which we observe as sinusoidal function in figure 3.

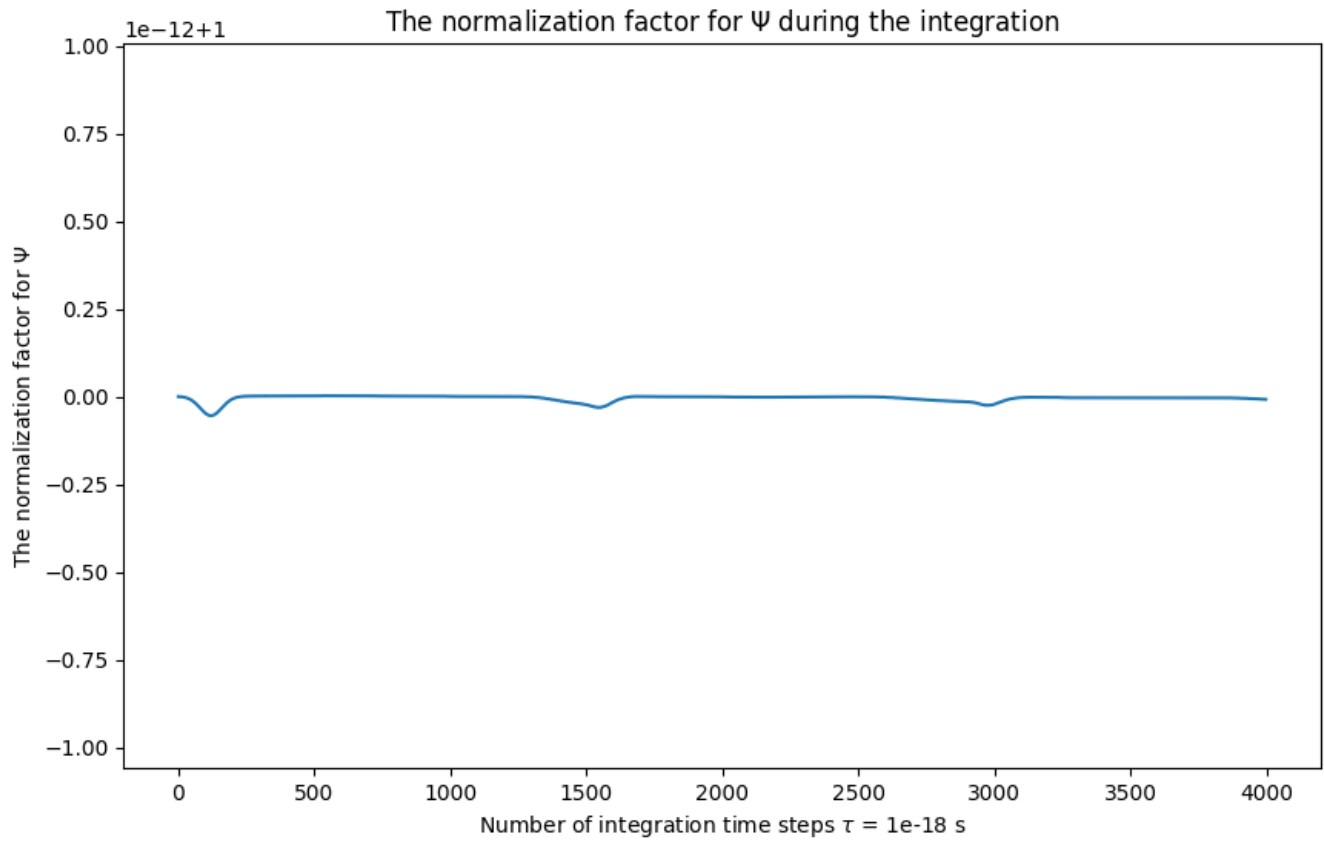


Figure 5: The normalization of the wave function through time in a harmonic potential.

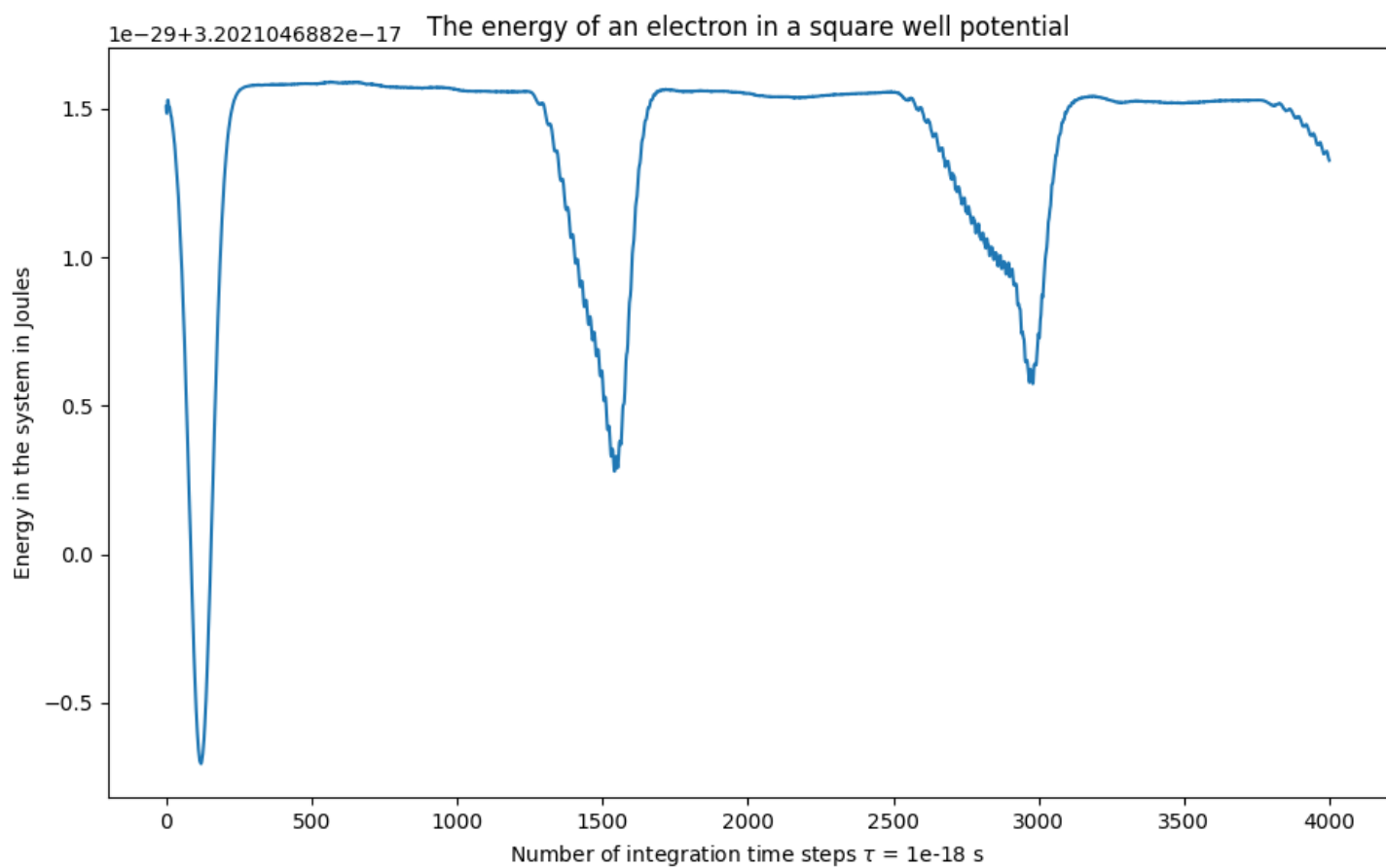


Figure 6: The energy of the system through time in a harmonic potential.



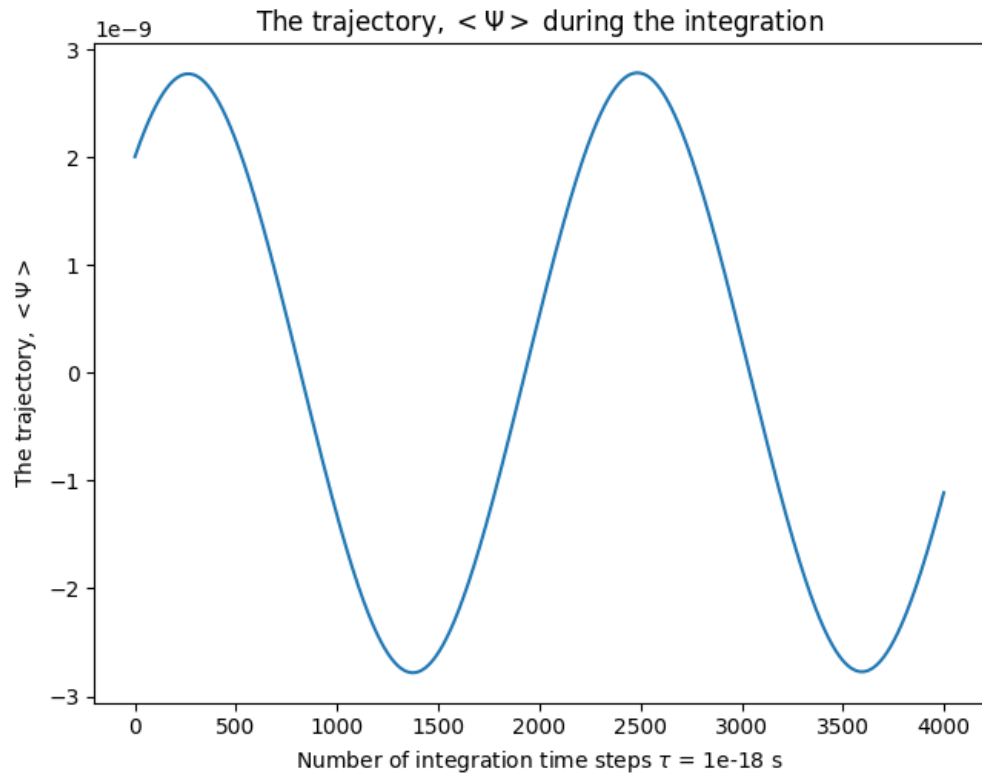


Figure 7: The trajectory of the wave function through time in a harmonic potential.

The probability density functions for 3000 time steps with  $\tau=1e-18$

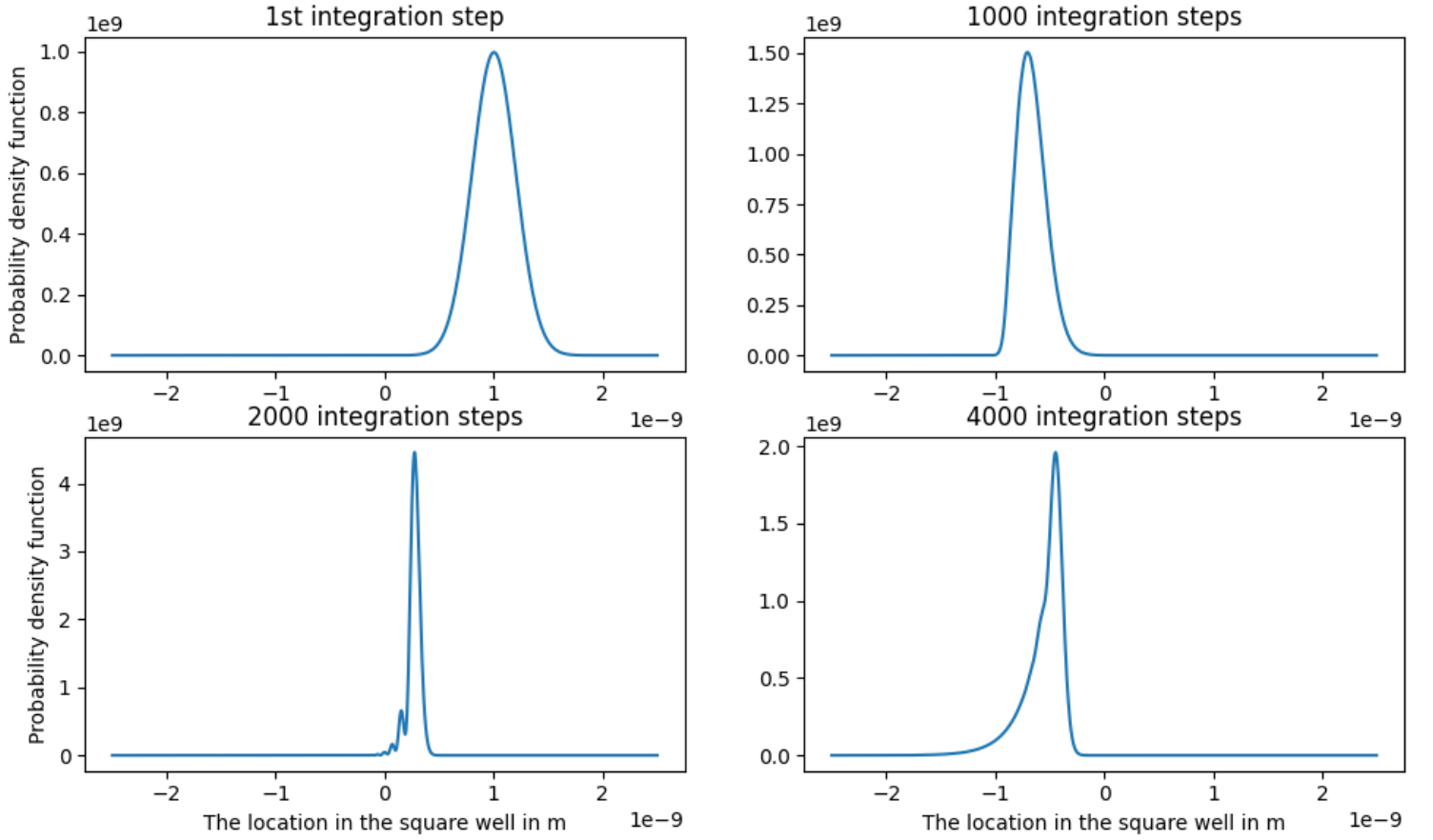


Figure 8: Snapshots of the probability density function for the position in a harmonic potential.

d)

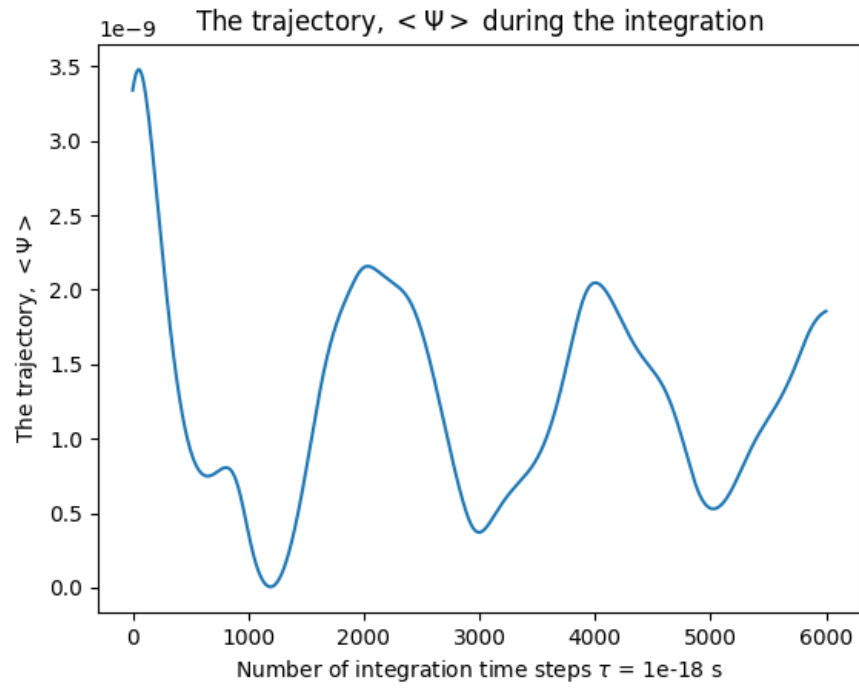


Figure 9: The trajectory of the wave function through time in a double well.

The probability density functions for 3000 time steps with  $\tau=1e-18$

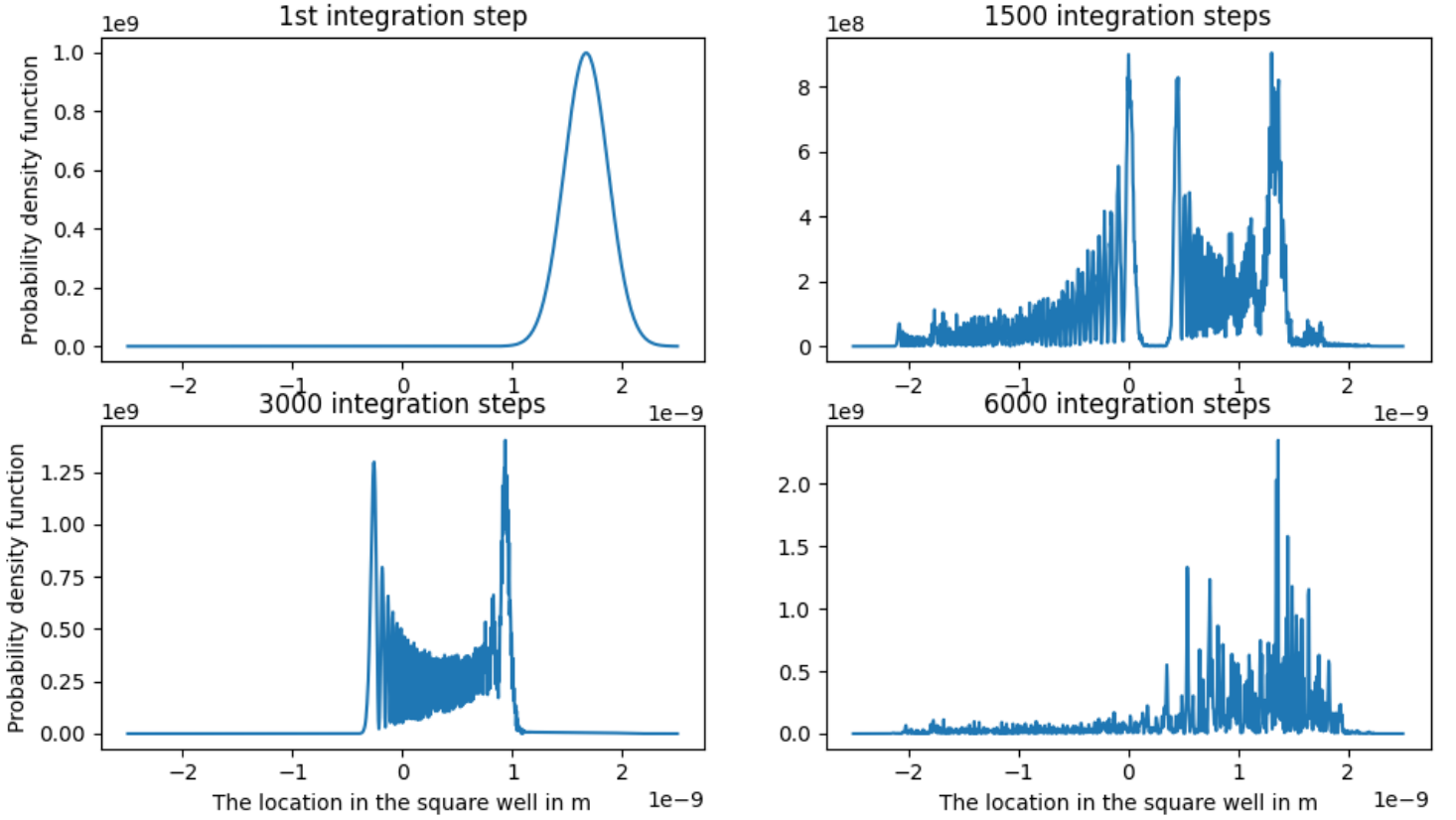


Figure 10: Snapshots of the probability density function for the position in a double well.

We are asked to modify our code to calculate the Schrodinger equation with a double well potential. We observe the trajectory of the wave function in figure 9 which does not appear to have a regular pattern. Examining our probability density function in figure 10 we notice that we do not have any sharp concentration around any one particular position for each time step, but is instead distributed with concentrations in multiple locations. Ehrenfest theorem does not indicate the type behaviour of the expected position or momentum. However looking at the expected position we can see that this system is not behaving classically.

## Question 2

a)

We are asked to show that the following decompositions:

$$(E_z)_{p,q}^n = \sum_{q'=0}^P \sum_{p'=0}^P \hat{E}_{p,q'}^n \sin\left(\frac{pp'\pi}{P}\right) \sin\left(\frac{qq'\pi}{P}\right) \quad (1)$$

$$(H_x)_{p,q}^n = \sum_{q'=0}^P \sum_{p'=0}^P \hat{X}_{p,q'}^n \sin\left(\frac{pp'\pi}{P}\right) \cos\left(\frac{qq'\pi}{P}\right) \quad (2)$$

$$(H_y)_{p,q}^n = \sum_{q'=0}^P \sum_{p'=0}^P \hat{Y}_{p,q'}^n \cos\left(\frac{pp'\pi}{P}\right) \sin\left(\frac{qq'\pi}{P}\right) \quad (3)$$

$$(J_z)_{p,q}^n = \sum_{q'=0}^P \sum_{p'=0}^P \hat{J}_{p,q'}^n \sin\left(\frac{pp'\pi}{P}\right) \sin\left(\frac{qq'\pi}{P}\right) \quad (4)$$

where  $P$  is the number of grid points, satisfy the following boundary conditions:

1.  $E_z = 0$  at  $x = 0, L_z$  and  $y = 0, L_y$
2.  $H_x = \partial_x H_y = 0$  at  $x = 0, L_x$
3.  $H_y = \partial_y H_x$  at  $y = 0, L_y$

### Checking Boundary Conditions

1. We check the boundary condition 1 with respect to Equation 1.

At  $x = 0$ ,  $p = 0$ . Thus,

$$(E_z)_{0,q}^n = \sum_{q'=0}^P \sum_{p'=0}^P \hat{E}_{0,q'}^n \sin\left(\frac{0p'\pi}{P}\right) \sin\left(\frac{qq'\pi}{P}\right) = 0$$

as  $\sin\left(\frac{pp'\pi}{P}\right) = 0$ .

Similarly, at  $y = 0$ ,  $q = 0$ ,  $\sin\left(\frac{qq'\pi}{P}\right) = 0$ ,  $(E_z)_{p,0}^n = 0$ .

At  $x = L_x$ ,  $p = P$ :  $\sin\left(\frac{pp'\pi}{P}\right) = \sin\left(\frac{pP'\pi}{P}\right) = \sin(p'\pi) = 0$  as  $p'$  is an integer.

At  $y = L_y$ ,  $q = P$ :  $\sin\left(\frac{qq'\pi}{P}\right) = \sin(q'\pi) = 0$  as  $q'$  is an integer. Thus, with reference to Equation 1,  $(E_z)_{p,q}^n = 0$  at  $x = L_x, y = L_y$ . Thus, the first boundary condition is satisfied.

2. We now check boundary condition 2. First we calculate  $\partial_x H_y$ :

$$\begin{aligned} \partial_x H_y &= \partial_x \left( \sum_{q'=0}^P \sum_{p'=0}^P \hat{Y}_{p,q'}^n \cos\left(\frac{pp'\pi}{P}\right) \sin\left(\frac{qq'\pi}{P}\right) \right) \\ &= \partial_x \left( \sum_{q'=0}^P \sum_{p'=0}^P \hat{Y}_{p,q'}^n \cos\left(\frac{xp'\pi}{L_x}\right) \sin\left(\frac{qq'\pi}{P}\right) \right) \text{ as } \frac{p}{P} = \frac{x}{L_x} \\ &= -\frac{p'\pi}{L_x} \sum_{q'=0}^P \sum_{p'=0}^P \hat{Y}_{p,q'}^n \sin\left(\frac{xp'\pi}{L_x}\right) \sin\left(\frac{qq'\pi}{P}\right) \end{aligned}$$

At  $x = 0$ ,  $\sin\left(\frac{xp'\pi}{L_x}\right) = 0$  and thus the condition  $\partial_x H_y = 0$  holds.

Similarly for  $x = L_x$ ,  $\sin\left(\frac{xp'\pi}{L_x}\right) = \sin(p'\pi) = 0$ .

Thus,  $\partial_x H_y = 0$  at  $x = 0, L_x$ .

We check  $H_x = 0$  at the vertical walls with respect to the sine term in Equation 2:

At  $x = 0 \Leftrightarrow p = 0$ ,  $H_x = 0$  as  $\sin\left(\frac{pp'\pi}{P}\right) = 0$  for all integers  $p'$ .

At  $x = L_x \Leftrightarrow p = P$ ,  $H_x = 0$  as  $\sin\left(\frac{Pp'\pi}{P}\right) = \sin(p'\pi) = 0$  for integers  $p'$ .

Thus,  $H_x = 0$  at the vertical walls at  $x = 0, L_x$ .

3. We calculate  $\partial_y H_x$

$$\begin{aligned}\partial_y H_x &= \partial_y \left( \sum_{q'=0}^P \sum_{p'=0}^P \hat{X}_{p,q'}^n \sin\left(\frac{pp'\pi}{P}\right) \cos\left(\frac{qq'\pi}{P}\right) \right) \\ &= \partial_y \left( \sum_{q'=0}^P \sum_{p'=0}^P \hat{X}_{p,q'}^n \sin\left(\frac{pp'\pi}{P}\right) \cos\left(\frac{yq'\pi}{L_y}\right) \right) \\ &= -\frac{q'\pi}{L_y} \sum_{q'=0}^P \sum_{p'=0}^P \hat{X}_{p,q'}^n \sin\left(\frac{pp'\pi}{P}\right) \sin\left(\frac{yq'\pi}{L_y}\right)\end{aligned}$$

At  $y = 0, L_y$ ,  $\sin\left(\frac{yq'\pi}{L_y}\right) = 0$ . Thus  $\partial_y H_x = 0$  at  $y = 0, L_y$ .

We check that  $H_y = 0$  at the horizontal walls with respect to the sine term in Equation 2. At  $y = 0 \Leftrightarrow q = 0$ ,  $H_y = 0$  as  $\sin\left(\frac{qq'\pi}{P}\right) = 0$ .

At  $y = L_y \Leftrightarrow q = P$ ,  $H_y = 0$  as  $\sin\left(\frac{qq'\pi}{P}\right) = \sin\left(\frac{Pq'\pi}{P}\right) = \sin(q'\pi) = 0$ . Thus,  $H_y = 0$  at  $y = 0, L_y$ .

**b)**

We are asked to write our own equations to compute the fourier transforms for Equations 1 to 4.

We first modify the 2-dimensional wave equations discrete sin and cos transform functions `dst2` and `dct2`, which correspond to Equations 1 and 4 respectively.

We modify these schemes to create `dsct2` and `dcst2` for Equations 2 and 3 respectively (and of course their inverses). For `dsct2`, we took the discrete cosine transform along the y-axis and the discrete sine transform along the x-axis. For `dcst2`, this is reversed. Their inverse are analogously created.

We do this within the provided `dsct.py` file which we renamed `Lab09_Q2b.py` as per naming convention.

**c)**

We are asked to implement our 2D Fourier transforms written for (b) into a python script that calculates  $E_z$ ,  $H_y$  and  $H_x$  for some time period  $T$ . We set the final time  $T = N\tau$ , where the time step  $\tau = 0.01$ . The dimensions of the problem are as follows,  $L_x = L_y = J_0 = m = n = c = 1$  and  $P = 32$ .

### Pseudocode

```
# Initialize constants L_x, L_y, J_0, m, b, c, P
# Initialize time array
# Compute D_x, D_y, a_x, a_y as per handout
```

```

# Initialize spatial grid with [x,y] coordinates
# Use spatial grid to compute the time-independent factor of J_z

# Initialize initial H_x, H_y, E_z, J_z for t = 0, into P+1 x P+1
# arrays

# Initialize accumulator arrays for E_z, H_x, H_y, J_z

# Create time_array to loop over

# Loop over time array
    # Obtain fourier coefficients for E_z, X, Y, and J_z

    # Use Crank Nicholson scheme to obtain the coefficients
    # for next step time + tau for fourierE_z, X and Y

    # Take the inverse fourier transform to obtain next step
    # E_z, H_x, and H_y in the spatial dimension

    # Compute next step J_z

    # Store next step E_z, H_x, H_y in accumulator arrays

    # update E_z, H_x, H_y, J_z using np.copy

# Plot

```

We code this routine in `Lab.09-Q2ce.py`, for  $\omega = 3.75$ . We are asked to provide plots for  $E_z(x = 0.5, y = 0.5)$  and  $H_y(x = 0.0, y = 0.5)$  and  $H_x(x = 0.5, y = 0.0)$ . We plot this superimposed onto the same figure in Fig 11. We see that  $H_x$  and  $H_y$  have the same waveform with respect to their axis.  $E_x$  has a similar magnitude and overall oscillatory pattern to  $H_x$  and  $H_y$ . We note that there may be interference occurring at the point  $(0.5, 0.5)$  causing pattern above. This would be the non-resonant case in the cavity.



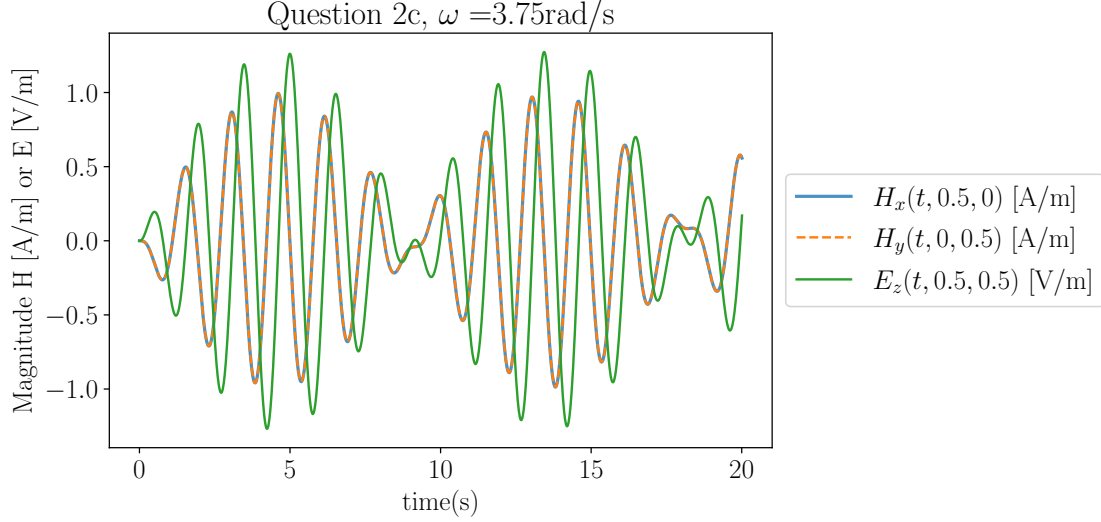


Figure 11: Plot of  $E_z(x = 0.5, y = 0.5)$  and  $H_y(x = 0.0, y = 0.5)$  and  $H_x(x = 0.5, y = 0.0)$  with respect to time. Note the oscillatory wavepacket-like pattern.

d)

We want to find the max amplitude of  $E_z(x = 0.5, y = 0.5, t)$  over a range of  $\omega$  from 0 rad/s to 9 rad/s, i.e. we want to find the driving frequency such that resonance occurs.

To do this, we plot maximum amplitude of  $E_z(x = 0.5, y = 0.5, t)$  against  $\omega$  from 0 to 9 rad/s.

We implement our routine for 2c but over a range of omegas and store the maximum amplitude to  $E_z$  at  $(x, y) = (0.5, 0.5)$ . To obtain the maximum amplitude for a given  $\omega$ , we take the maximum of absolute values of the entries the 1-dimensional array associated with  $E_z(x = 0.5, y = 0.5, t)$ . We can do this as the equilibrium magnitude of the wave appears to be at  $E_z(0.5, 0.5, t) = 0$ .

Our values of omega we use are from 0 to 9 with a step of 0.1. To save computational time, one may want to change this to 0.5 under the variable `domega`.

Our script can be found in `Lab09_Q2d`. Our plot can be obtained in Fig 12. We note a spike occurs at  $\omega = 4.5 \text{ rad/s}$ . Comparing this to the equation for the normal frequency with mode  $m, n = 1$  with our constants  $L_x, L_y, c = 1$  as per our script routine:

$$\omega_0^{1,1} = \pi c \sqrt{(nL_x)^{-2} + (mL_y)^{-2}} = \pi 1 \sqrt{(1)^{-2} + (1)^{-2}} = 4.443 \text{ rad/s}$$

We can see the spike in amplitude corresponds to the  $m = 1, n = 1$  normal frequency mode.

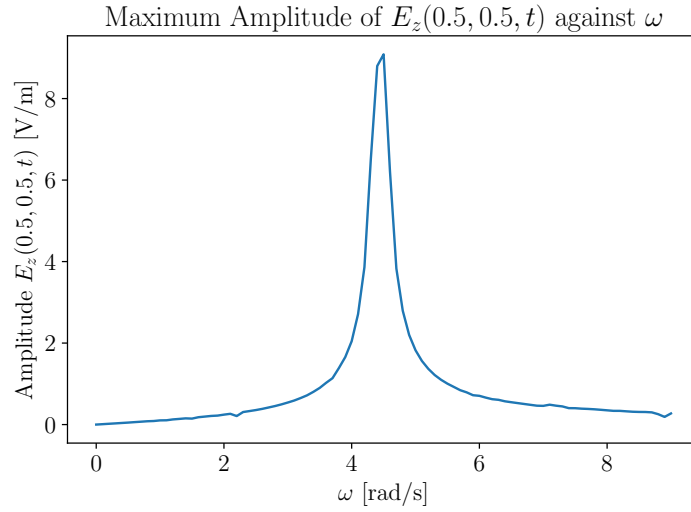


Figure 12: Plot of max amplitude of  $E_z(x = 0.5, y = 0.5)$  [V/m] against  $\omega$  [rad/s]. Note the spike at  $\omega = 4.5$  rad/s.

e)

We repeat our routine for question 2c, but this time with  $\omega = \omega_0^1, 1$ . We plot  $E_z(x = 0.5, y = 0.5)$  and  $H_y(x = 0.0, y = 0.5)$  and  $H_x(x = 0.5, y = 0.0)$  in Fig 13. We see that  $E_z$ ,  $H_y$  and  $H_x$  have increasing amplitudes over time, an indicator of resonance occurring within the cavity. We can say that for this frequency, at this point  $x = 0.5$  and  $y = 0.5$ , energy of the B-field and E-field is increasing. W

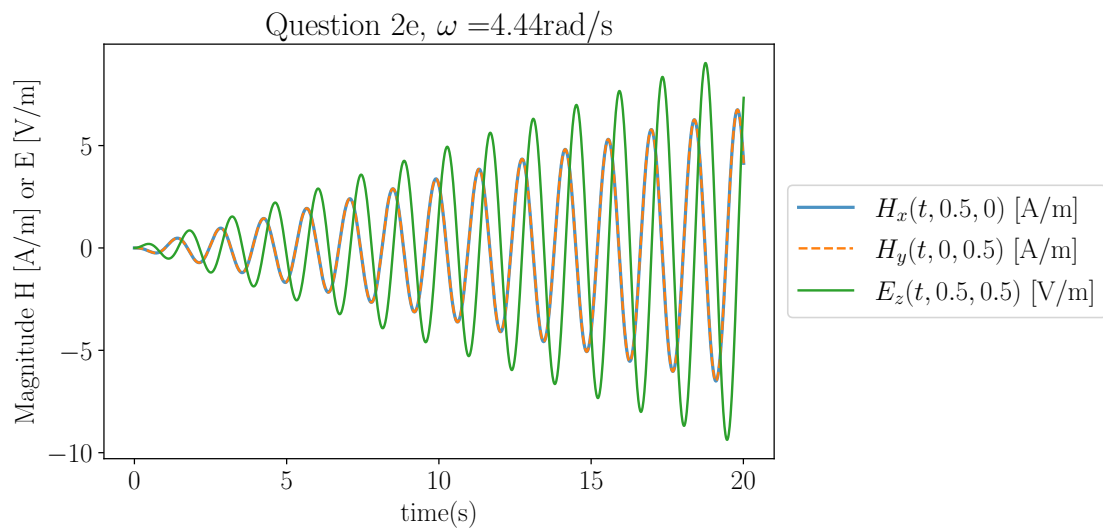


Figure 13: Plot of max amplitude of  $E_z(x = 0.5, y = 0.5)$  [V/m] against  $\omega$  [rad/s]. Note the spike at  $\omega = 4.5\text{rad/s}$ .